Bollettino di Geofisica Teorica ed Applicata Vol. 53, n. 4, pp. 485-508; December 2012
DOI 10.4430/bgta0048

# Coupled seismogenic geohazards in Alpine regions

D. Fäh, J.R. Moore, J. Burjanek, I. Iosifescu, L. Dalguer, F. Dupray, C. Michel, J. Woessner, A. Villiger, J. Laue, I. Marschall, V. Gischig, S. Loew, A. Marin, G. Gassner, S. Alvarez, W. Balderer, P. Kästli, D. Giardini, C. Iosifescu, L. Hurni, P. Lestuzzi, A. Karbassi, C. Baumann, A. Geiger, A. Ferrari, L. Laloui, J. Clinton and N. Deichmann

*Swiss Seismological Service, ETH, Zürich, Switzerland*

(Received: May 17, 2011; accepted: October 24, 2011)

***ABSTRACT*** COupled seismogenic GEohazards in Alpine Regions (COGEAR) is an interdisciplinary natural hazard project investigating the hazard chain induced by earthquakes. It addresses tectonic processes and the related variability of seismicity in space and time, earthquake forecasting and short-term precursors, and strong ground motion as a result of source and complex path effects. We study non-linear wave propagation phenomena, liquefaction and triggering of landslides in soil and rock, as well as earthquake-induced snow avalanches. The Valais, and in particular parts of the Rhone, Visper, and Matter valleys have been selected as study areas. Tasks include detailed field investigations, development and application of numerical modeling techniques, assessment of the susceptibility to seismically induced effects, and installation of different monitoring systems to test and validate our models. These systems are for long-term operation and include a continuous GPS and seismic networks, a test installation for observing earthquake precursors, and a system to study site-effects and non-linear phenomena in two test areas (Visp, St. Niklaus / Randa). Risk-related aspects relevant for buildings and lifelines are also considered.

**Key words:** seismic ground motion, non-linear phenomena, landslides, earthquake precursors, earthquake forecasting, Switzerland.

## 1. Introduction

The region of Canton Valais (Fig. 1) has the highest seismic hazard in Switzerland, experiencing a magnitude 6 or larger earthquake roughly every 100 years (1524, 1584, 1685, 1755, 1855, 1946). In particular, the area near Visp holds special interest, as damaging earthquakes occur on average every 40 years (intensity VI-VIII) with the most recent in 1960 reaching a macroseismic intensity of VII (Fäh *et al.*, 2011). The Visp earthquake of 1855 was the largest in Switzerland during the last 300 years. Although the temporal occurrence of strong earthquakes in the area was regular in past centuries, instrumental seismicity of the last decades presents a peculiar spatial pattern (Fig. 1). For example, we observe a high seismic activity in the region of the 1946 $M_W$=5.8 earthquake, whereas a seismic quiescence in the area of 1755 $M_W$=5.7 and 1855 $M_W$=6.2 events. Thus, it is now important more than ever to assemble seismic and geodetic observations to understand ongoing tectonic processes. Differences in seismicity between northern and southern Valais manifest themselves both by the style of faulting and changes in the stress field orientation. In addition to high seismic activity, the Valais has several factors adding to the

 

total hazard level: rough topography, unstable and steep slopes, deep sediment-filled valleys, and wide glacier- and snow-covered areas. The area has experienced significant damage and induced effects from strong ground motion during previous large earthquakes, which also included secondary phenomena such as liquefaction in the Rhone plain, deep-seated landslides, and extensive rockfalls.

A major goal for the Valais is interdisciplinary investigation of short- and long-term earthquake preparation processes, in addition to complex surface effects induced by strong ground motion. These concepts are addressed in the research project "COupled seismogenic GEohazards in Alpine Regions" (COGEAR, http://www.cogear.ethz.ch), supported by the Competence Center for Environment and Sustainability (CCES) of the ETH Domain. The project investigates tectonic processes and related variability of seismicity in space and time, earthquake forecasting and observation of possible short-term precursors, and modeling and observation of weak and strong ground motion as a result of complex source and path effects. We study non-linear wave propagation phenomena and liquefaction in soils, wave propagation instable rock and soil slopes, the long-term impacts of repeated earthquakes on slope stability through strength degradation, and triggering of landslides and snow avalanches. A multi-sensor monitoring system forms the foundation of our research activities, which builds on existing networks and includes installation of new equipment. The planned multi-sensor network includes:

1) a dense regional sensor network for monitoring crustal deformation, seismicity, and possible active faults in the Valais, including seismic stations in boreholes;
2) local strong-motion networks for monitoring earthquake ground motion and 3D site-effects in Visp, St. Niklaus, and Grächen;
3) test sites for studying site-effects, non-linear phenomena in liquefiable soils and related pore pressure effects in Visp;
4) test sites to study site-effects and dynamic loading of landslides in relation to topography, geological disposition, kinematics and slope stability;
5) installations to monitor possible short-term earthquake precursors, including electromagnetic and geo-chemical sensors;
6) seismic monitoring of buildings in the Visp area at a later stage.

These systems are planned to be operational for several decades, and the probability is high that they will capture the next damaging earthquake in the Valais. All project data are combined in a common geo-referenced platform, which is accessible via a new web interface. The monitoring system and subsequent data analysis lays the foundation for development of new tools for real-time seismic hazard assessment.

## 2. Multi-sensor instrumentation in the Valais

In order to verify numerical models and improve our observational possibilities, a large number of instruments is installed in the multi-sensor network of COGEAR. The present status and plan for the full monitoring system is outlined in Fig. 2. Densification of the high-gain seismic network in the region is now complete. With the new stations, the seismic network is capable of locating earthquakes in the study area down to very low magnitudes. GPS stations are co-located at a number of these sites. The seismic stations are complemented by a network of new strong motion

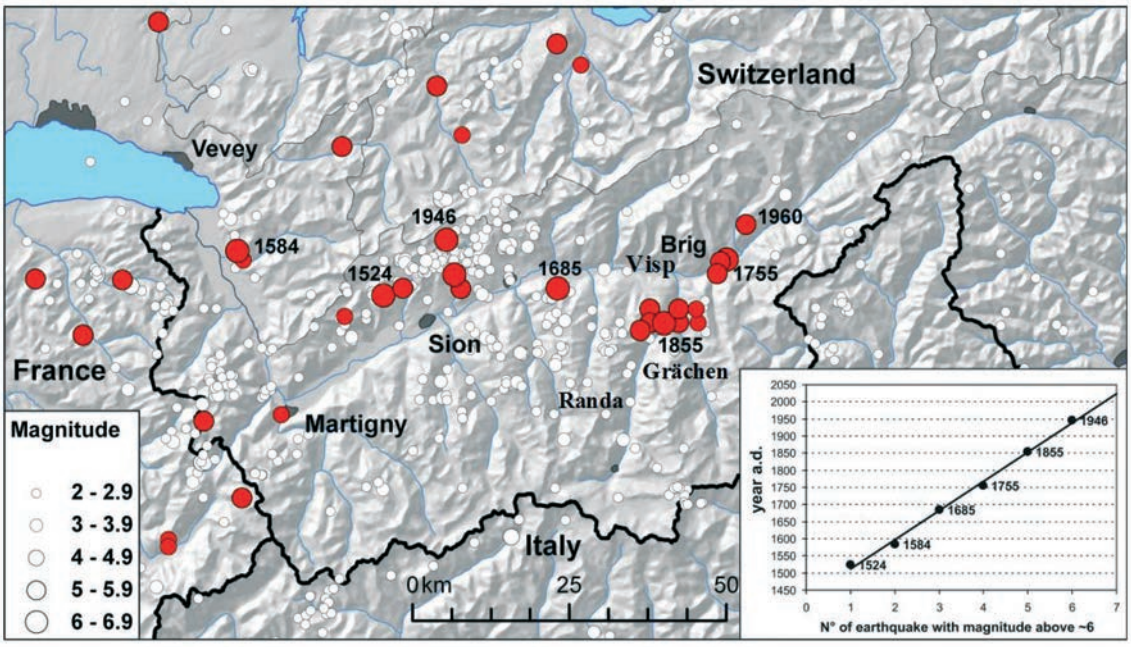


Fig. 1 - Seismicity in the Valais. Recurrence of the earthquakes with intensity equal to VIII is depicted in the inset (bottom right).

sensors in Visp and the Matter valley, which are used to test ground motion prediction models and for three-dimensional ground motion modeling. A borehole site has been identified in Visp where seismic instruments at different depths, as well as deformation devices, will be installed in 2012. For monitoring of unstable rock slopes, a new fiber optic strain measurement system was installed at the Randa in-situ laboratory, which is able to detect micro-strain deformations at 100 Hz triggered sampling. Finally, a specially designed fluorometer was installed at the Brigerbad thermal spring, which continuously measures fluorescence over three channels of different wavelengths together with the turbidity of the water. Additionally, water temperature, $CO_2$, $CH_4$ and Radon are measured at the same time intervals as the other parameters. The goal is to detect any geochemical changes that could precede intermediate and large earthquakes. This geochemical installation is part of a permanent multi-sensor network for detection of non-seismic, short-term earthquake precursors, also including planned electromagnetic sensors. Further details of the different sensing systems can be found in the following sections.

## 3. Database and data exchange

An important aspect of COGEAR is to integrate in a systematic and coherent manner all research data, including sensor information and large supporting topographic and geological data sets. Due to the heterogeneous nature of project data sets, the COGEAR data exchange was designed with a generic, distributed architecture (Fig. 3). The architecture has three components, namely a data management component, a computation component, and an interaction component,

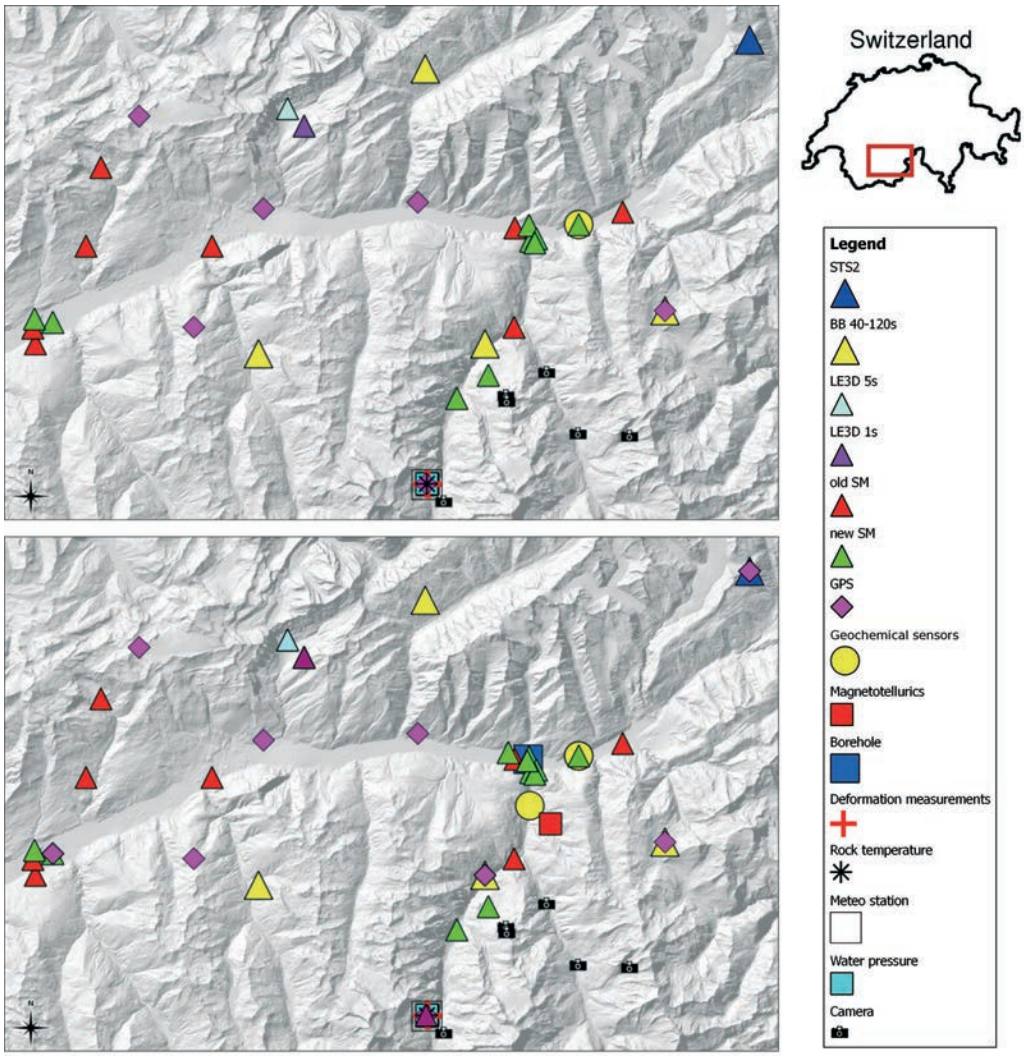


Fig. 2 - Present status of sensors in 2011 (top), and plan for the full monitoring system at the end of COGEAR (bottom). Location of the area is represented as a box on the map of Switzerland (top right). Seismic stations are represented by triangles (BB: broadband sensors; LE3D Lennartz three-component sensor; SM: strong motion sensor). The symbol of camera represents sites equipped with time-lapse cameras for monitoring unstable rock-slopes.

which correspond to the data tier, logic tier, and presentation tier of the well-known three-tier architecture (Eckerson, 1995). The data tier is represented by several distributed databases, the application tier is represented by services (Web Map Services, Web Feature Services, Global Sensor Networks and Geoprocessing Services) for visualization and download, and the presentation tier is represented by the user interface (Iosifescu and Hurni, 2010).

For spatial data management, it is widely accepted that geo-spatial databases offer accurate data retrieval that provides the basis for reliable interdisciplinary research (Gogu *et al*., 2006). However, in a multidisciplinary environment, researchers perform data acquisition differently and many software packages and different data formats are used. These formats and procedures are best

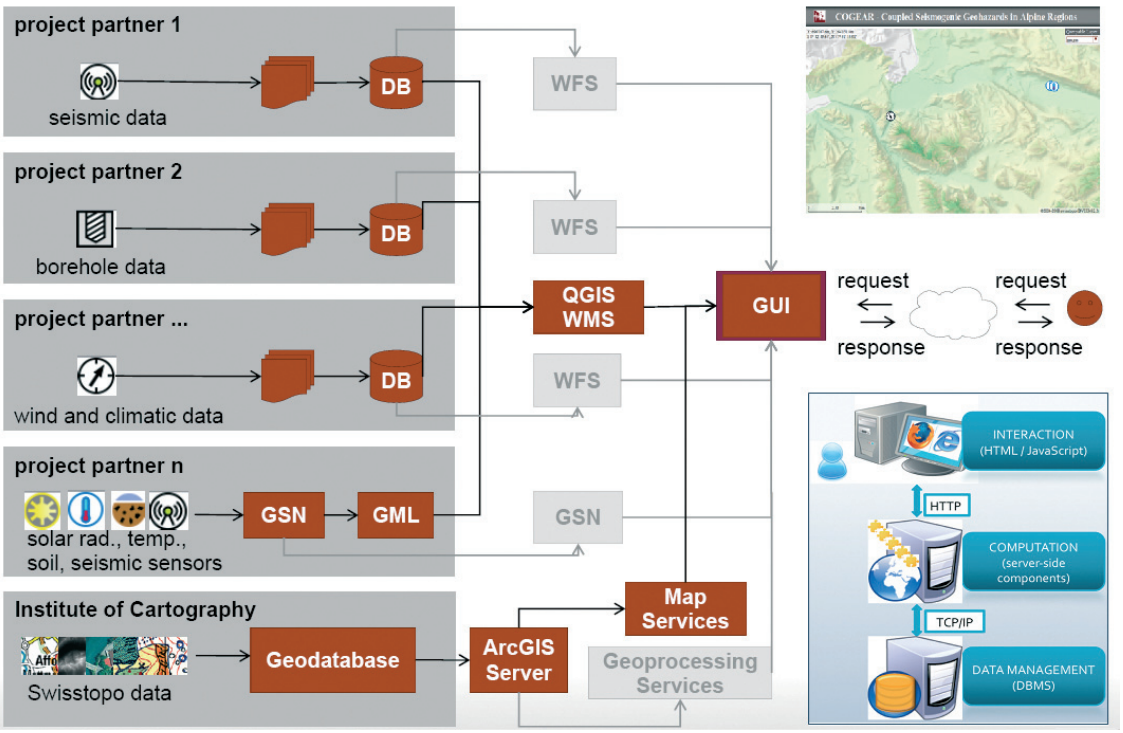


Fig. 3 - COGEAR data exchange architecture.

suited for the established intentions and it is not desired to modify the individual workflows (Iosifescu and Hurni, 2010).

The solution to this situation was to add the database management system layer on top of the established workflow. Researchers can acquire data, create models, perform simulations and obtain results in different ways, but it is mandatory to structure input data and final results in a database management system (DBMS) in order to profit from the advantages offered by a database in terms of data structuring and retrieval. The project partners agreed to implement PostgreSQL databases (PostgreSQL, 2011) due to its proven stability, compatibility with open-source GIS software, and the free and open-source status. Introduction of the databases to the individual institutions was not effortless. The methodology consisted of training research partners to develop and implement the databases in two separate steps. The first step included the training necessary to specify a database schema for existing data. The second step was to implement the schema in the database and incorporate data.

In addition to project-specific data, a database for large geological and topographical datasets was created in order to support research activities (Iosifescu and Hurni, 2010). Such data sets include geological maps, digital terrain models, and satellite imagery for all of Switzerland, in addition to the latest products of the Swiss National Mapping Agency, namely two digital elevation models of the surface and terrain (DOM and DTM-AV) and latest high-resolution airborne imagery from Swissimage. DOM and DTM-AV are high-precision modeling of the Earth's surface

below 2000 m based on airborne laser scanning, while Swissimage is a high-resolution aerial orthophoto mosaic with a ground pixel size of 25 cm.

Based on the distributed data tier, a two-step service provision workflow was designed and implemented. In the first step, web map services (WMS) were offered on top of the distributed data sources. In the second step, geo-processing services (GP services) and web feature services (WFS) were implemented to offer on-demand download of data sets from a specific area. Download services allow interactive selection of the area of interest, followed by data extraction (clipping) from the source and provision of a temporary download link. The workflow integrates all sensor data and metadata.

This workflow is based on the Geographic Mark-up Language (GML) for the exchange of sensor information and an extended WMS server, namely the QGIS mapserver (QGIS mapserver, 2011). QGIS mapserver is an open-source web map services implementation, which contains advanced cartographic features such as diagrams, patterns and custom symbols offered through an extended service interface (Iosifescu *et al.*, 2010). GML is an XML-based geospatial standard developed by the Open Geospatial Consortium, which is widely accepted for spatial data exchange and is also used by WFS. GML contains a rich set of primitives such as feature or geometries, which are used to build application-specific schemas or application languages, and in our case are automatically adapted for exchanging seismological, geological, and geotechnical data.

Finally, the service-oriented approach applied in the computation tier allows any graphical user interface (GUI) to interact with the visualization and download services by a simple request-response mechanism. The GUI sends a request to the web service and the server returns a response to the consumer containing the expected content (map or data). Therefore it is possible to use any cartographic GUI framework designed for the web browser. The COGEAR GUI prototype shown in Fig. 4 is based on the cartographic framework developed in the GeoVITe project (GeoVITe, 2011). The framework is free and open-source (Carto.net, 2011). Officially launched in January 2011, the COGEAR GIS platform allows for organizing and accessing research data in an intuitive manner, thus becoming an integral tool for interdisciplinary research and collaboration.

## 4. Results from seismotectonic and geodetic analysis

### *4.1. Seismotectonics*

The Valais is the most seismically active area in Switzerland. Earthquake epicenters in northern Valais follow a more or less ENE-WSW trending alignment situated north of and parallel to the Rhone Valley, while in the southern Valais (Switzerland) and in Haute Savoie (France) seismicity is more scattered (Fig. 5 top). The area is composed of two main tectonic units: the Helvetic domain in northern Valais and in most of the Haute Savoie, and the Penninic domain in southern Valais. In the northern Valais and Haute Savoie, earthquake focal mechanisms are predominantly strike-slip with P-axis orientations mainly NW-SE, while in the southern Valais they show normal faulting with T-axes oriented in a N-S direction. Active fault planes could be identified for 12 different earthquake sequences (Mauvoisin, two sequences of Anzère, Gd. Bornand, Leukerbad, Annecy, Samoëns, Martigny, Glarey, Derborence, Vallorcine and Sierre; Fig. 5 bottom) by applying a precise relative location procedure (e.g., Maurer and Deichmann, 1995; Maurer *et al.*, 1997; Fréchet *et al.*, 2011).

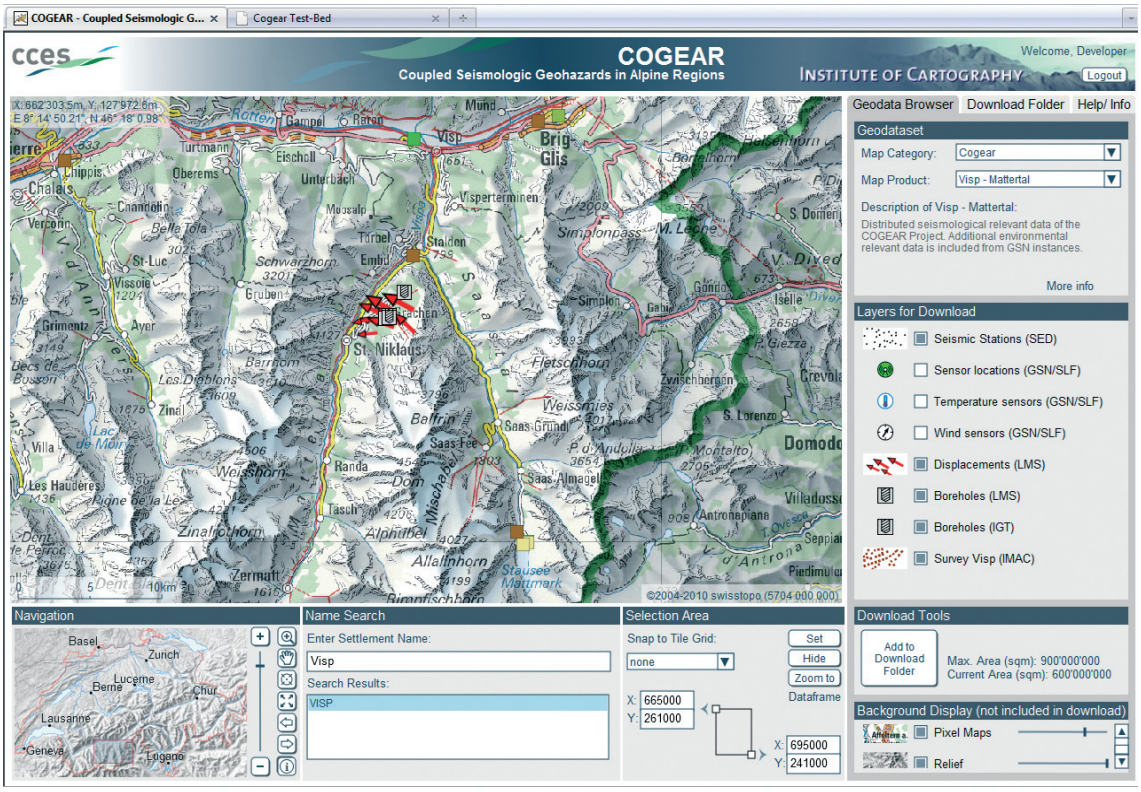


Fig. 4 - COGEAR GIS platform development prototype; © Institute of Cartography & COGEAR partners; base-map reproduced with authorization from Swisstopo (JA100120). Source: Bundesamt für Landestopographie swisstopo (Art. 30 GeoIV): 5704 000 000.

At first glance, the orientations of active fault planes identified in the Helvetic domain and in the Aiguilles Rouges Massif seem unsystematic. However, on a regional scale they are compatible with a rotation of the direction of maximum compression from E-W oriented compression south of the Lake of Geneva to NW-SE oriented compression in the Helvetic domain of northern Valais. On a local scale, this would mean that some of the identified fault planes are unfavorably oriented for rupture. Comprehensive analysis of the state of stress in the region based on focal mechanisms available up to 1998 was published by Kastrup *et al.* (2004). An update of this analysis incorporating newer data is currently underway.

### *4.2. Results from geodetic surveys*

Beginning in 1988, the Federal Office of Topography (Swisstopo) established a new national first-order GPS-based reference network LV95 (Landesvermessung, 95), in addition to constructing a permanent GPS reference network (AGNES) consisting of 34 stations. Three of the permanent stations are located in canton Valais (MART, HOHT, ZERM; see Fig. 6). The institute of Geodesy and Photogrammetry at ETH Zürich expanded the network from 2005 to 2006 in the framework of project TECVAL, which focused on the Wildstrubel area north of the Rhone Valley. Five sites with new geodetic GPS instrumentation (Trimble NetRS receiver and Zephyr antenna)

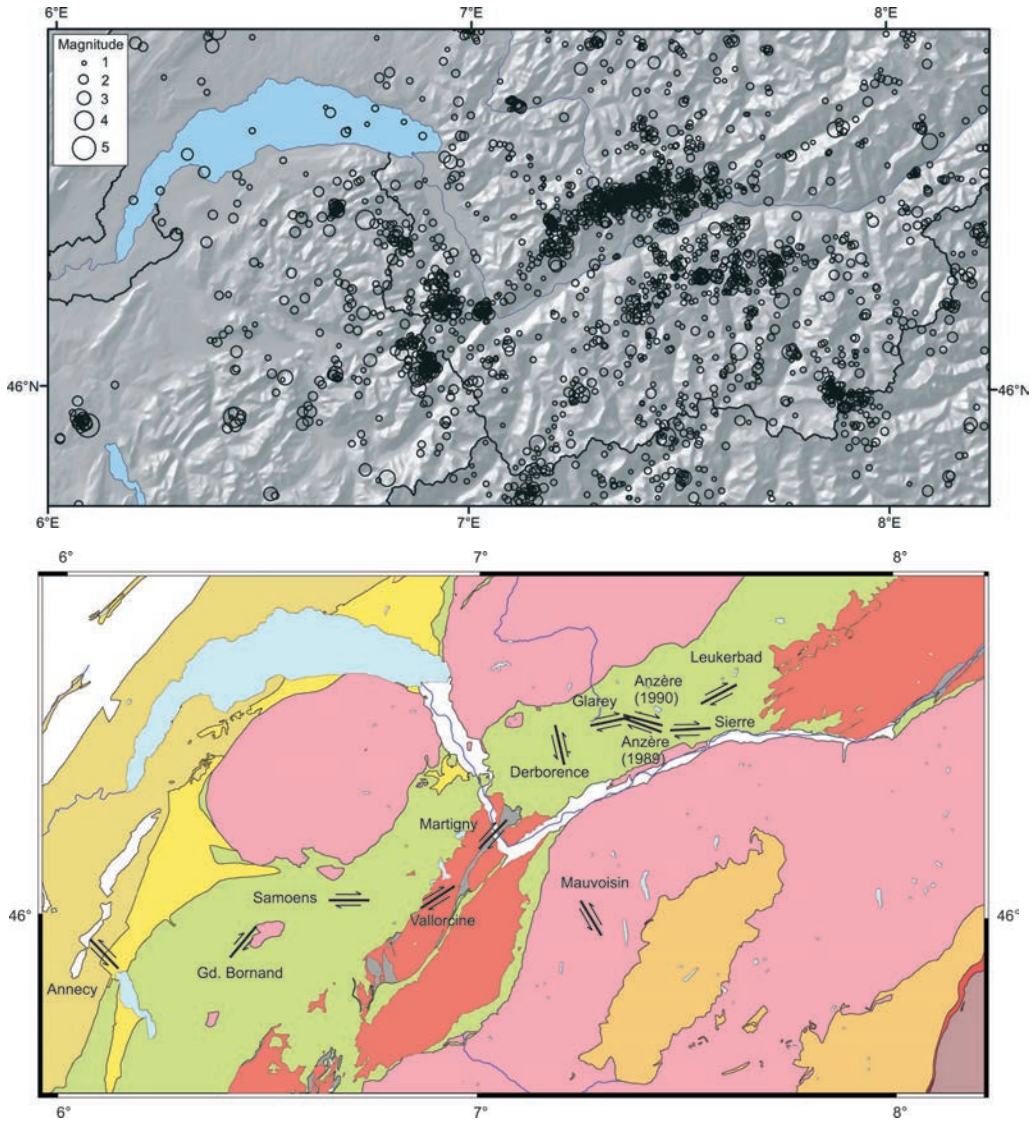


Fig. 5 - Top: earthquake epicenter map for the Valais (CH) and Haute Savoie (F) between 1984 and 2010 with ML>1.0. Bottom: tectonic map of the Valais (CH) and Haute Savoie (F) and orientation and slip of those active focal mechanism fault planes identified from precise relocations of earthquake sequences. Note that the dimensions of the fault planes are not to scale.

are operated permanently. Data from three of these stations are transferred to Swisstopo and included into automated analysis of the AGNES network (ERDE, VARE and WEHO; Fig. 6). To obtain better coverage around the area of Visp and the Matter valley, new permanent GNSS sites are planned consisting of a Leica GPRX1200+ receiver and AR25 choke-ring antenna. Use of choke-ring antennas will reduce multi-path effects and improve accuracy, which is vital since the expected relative annual displacements are small (mm range). When possible, GPS sites have been co-located with seismic stations. For velocity estimation with reasonable accuracy, observations

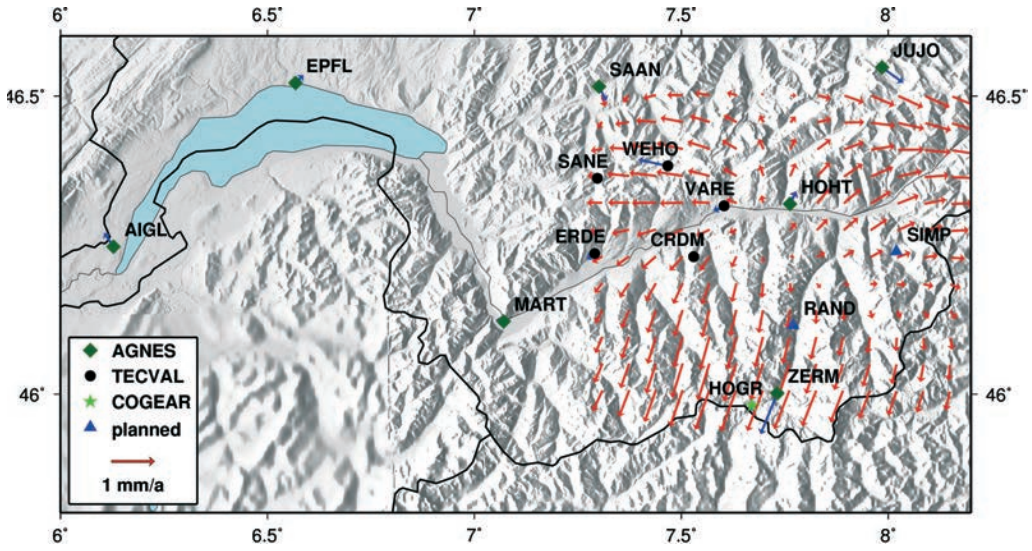


Fig. 6 - Preliminary velocity field (red arrows) derived from velocities calculated by Swisstopo (blue arrows). Stations CRDM and SANE are not included in the interpolation. Existing and planned continuous GNSS stations: project AGNES (diamond), TECVAL (circle), COGEAR (star), and planned (triangle).

must be recorded for several years to precisely determine and reduce seasonal effects and increase the reliability of the obtained results (Hollenstein *et al.*, 2008). Preliminary results of an interpolated velocity field are shown in Fig. 6. GPS data have been processed by Swisstopo using Bernese GPS software (Dach *et al.*, 2007). When velocities from all sites are available, local deformation will be better constrained and detailed comparisons with earthquake focal mechanisms possible.

### *4.3 Potential earthquake sources for ground motion prediction*

Evaluation of current seismic activity and the seismotectonic regime in the area around Visp suggests normal faulting as the predominant faulting mechanism. Guided by geological observations in this area, we have performed ambient noise seismic surveys along the trace of a potentially active fault (Fig. 7). This survey aimed at identifying evidence of brittle rock damage that may have evolved over repeat earthquake cycles through theoretical, geological, and seismological observations. Results indicate that a flower-like structure has formed near the free-surface of the fault, with significant shallow damage that decreases in magnitude and width with depth (e.g., Ben-Zion *et al.*, 2007). Results further show low amplitudes in the spectra of ambient noise along the cross-section of the expected fault zone, indicating a low-velocity zone corroborated by geological field studies (Fig. 7). The identified fault is in agreement with geological information from the area, e.g., from a recently drilled tunnel just below the measurement site. Seismological observations are used to constrain the fault location and narrow down the focal mechanism, in order to develop realistic rupture models. The recently installed strong-motion network may further help constraining the geometry of the fault by improving the precision of earthquake locations. Fig. 7 also shows an example of a possible fault rupture model for a magnitude ~6.5 earthquake in the Visp area, which will be used to simulate near-source

ground motion and assess spatial variability.

## 5. Time-dependent seismic hazard assessment and hazard products

Short-term earthquake forecasting and hazard assessment in general targets to better describe time-varying seismicity and earthquake hazard in a defined study area. A variety of such models have been developed for seismically active regions such as California and Italy, e.g., the Short-Term Earthquake Probability (STEP) (Gerstenberger *et al.*, 2005) and the Epidemic Type Aftershock Sequence (Ogata, 1998) models, and implemented in multiple variations (e.g., Woessner *et al.*, 2011 and references therein) in retrospective and prospective forecast testing experiments. In the framework of COGEAR, we worked on modifying the STEP-model to provide a well-constrained, time-varying seismicity forecast in a low-seismicity region and, in addition, to estimate the related hazard in terms of exceeding a given ground motion intensity comparable to results provided in long-term hazard models (Wiemer *et al.*, 2008).

We extended model developments initiated during the EU-FP6 project "Seismic Early Warning for Europe" (SAFER, www.safernetproject.org) for real-time forecasts in regions of low-seismicity rates such as Switzerland. In particular, the instrumentation of COGEAR added an important component for real-time forecasting, as improved seismic networks detecting small magnitude earthquakes with high reliability and low completeness threshold enable better estimation of parameters for forecast models. In addition, the availability of the earthquake catalogue of Switzerland [ECOS-09: Fäh *et al.* (2011)] enabled us to better constrain initial parameters of the model.

We implemented two model versions delivering real-time forecasts covering Switzerland for earthquakes of $M$>3.0. Both models rely in part on parameters for the Gutenberg-Richter and the Omori-law estimated for Italy by Gasperini and Lolli (2006): 1) a STEP-model based on Woessner *et al.* (2010) that resembles the procedures of the model implementation for California (Gerstenberger *et al.*, 2005), and 2) a model that parameterizes the abundance of aftershocks based on Christophersen and Gerstenberger (2010). The abundance model is of particular interest because the parameter calibration for seismicity relations of aftershock sequences, such as the Omori-law, in low-productivity regions is problematic. Both models still need improvement, however, as the first implementation likely forecasts seismicity rates that are too high, while the second model likely underestimates seismicity rates. The models are implemented and retrospective tests have shown that the cumulative forecast is acceptable. Forecast testing and investigation of new functional forms for the abundance model are ongoing.

Based on the seismicity rate forecasts, we generate time-dependent hazard maps that show the probability of exceeding an EMS-98 intensity level V in the next 24 hours using the ground motion prediction equation of Fäh *et al.* (2003). Such maps are provided for soft rock and estimated site amplifications based on Kästli and Fäh (2008). Fig. 8 displays an example of the time-dependent hazard levels expected following the September 8, 2005 $M_L$=4.9 Vallorcine earthquake with (bottom) and without (top) site amplification. Site amplification factors strongly influence the spatial distribution of predicted hazard values.

In summary, developing short-term earthquake forecast models for Switzerland and the Valais remains a challenge due to the low seismicity rate. The extension of the seismic network

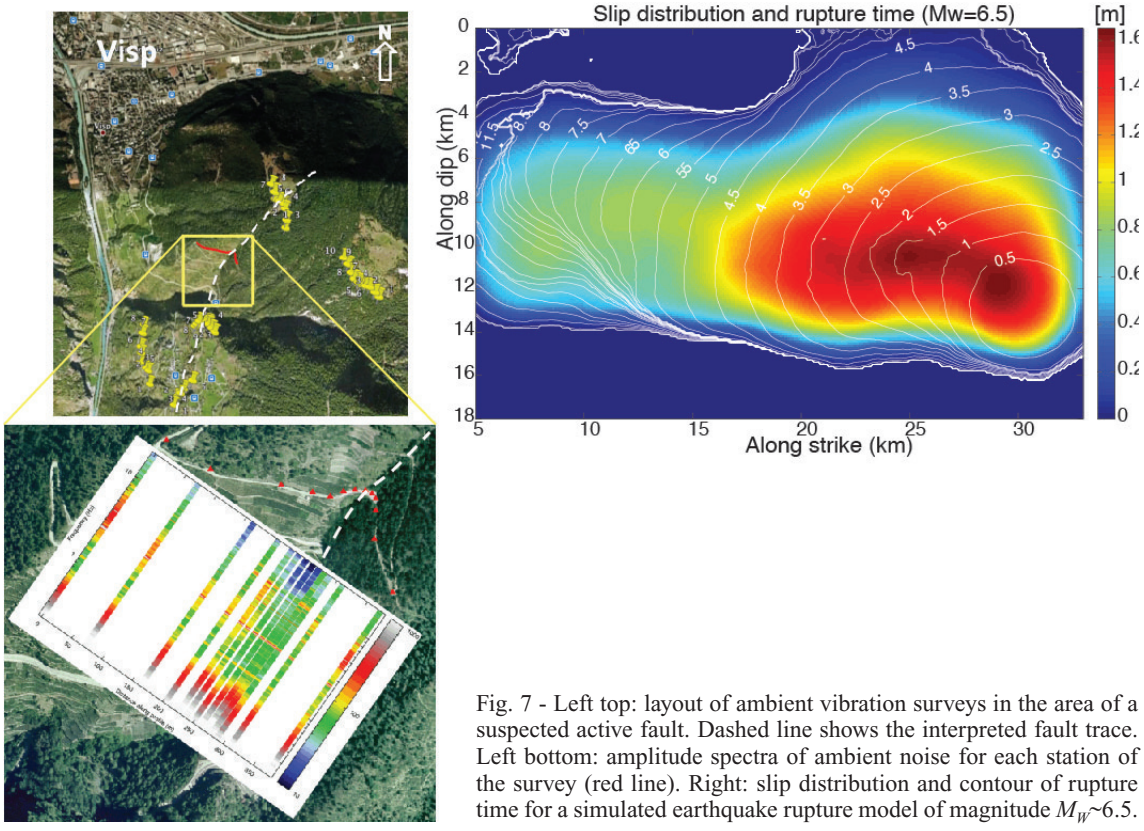


Fig. 7 - Left top: layout of ambient vibration surveys in the area of a suspected active fault. Dashed line shows the interpreted fault trace. Left bottom: amplitude spectra of ambient noise for each station of the survey (red line). Right: slip distribution and contour of rupture time for a simulated earthquake rupture model of magnitude $M_W$~6.5.

performed within COGEAR has contributed to the improvement of these types of models. Nevertheless, a full benefit is expected in the future as new data will help to improve the initial model parameters.

## 6. Site response analysis and vulnerability assessment for Visp

One final goal of the project COGEAR is to provide detailed damage scenarios. We therefore intend to combine the modeling of realistic source effects discussed in section 4, the 3D linear and non-linear soil response, and the vulnerability of the structures. In the following sections we present the basic input together with the level of detail we intend to obtain in the scenario modeling.

### *6.1. 3D Model for simulation of strong ground motion*

Due to river regulations and engineering progress over the last two centuries, seismically unfavorable sites within the Rhone valley have been expanded for settlement and industry. However, it is known that the area of modern Visp experienced soil liquefaction, ground failures, and generally heavy shaking during the 1855 earthquake (Fritsche *et al.*, 2006). As there are no available instrumental observations of these phenomena for the region, numerical modeling is the

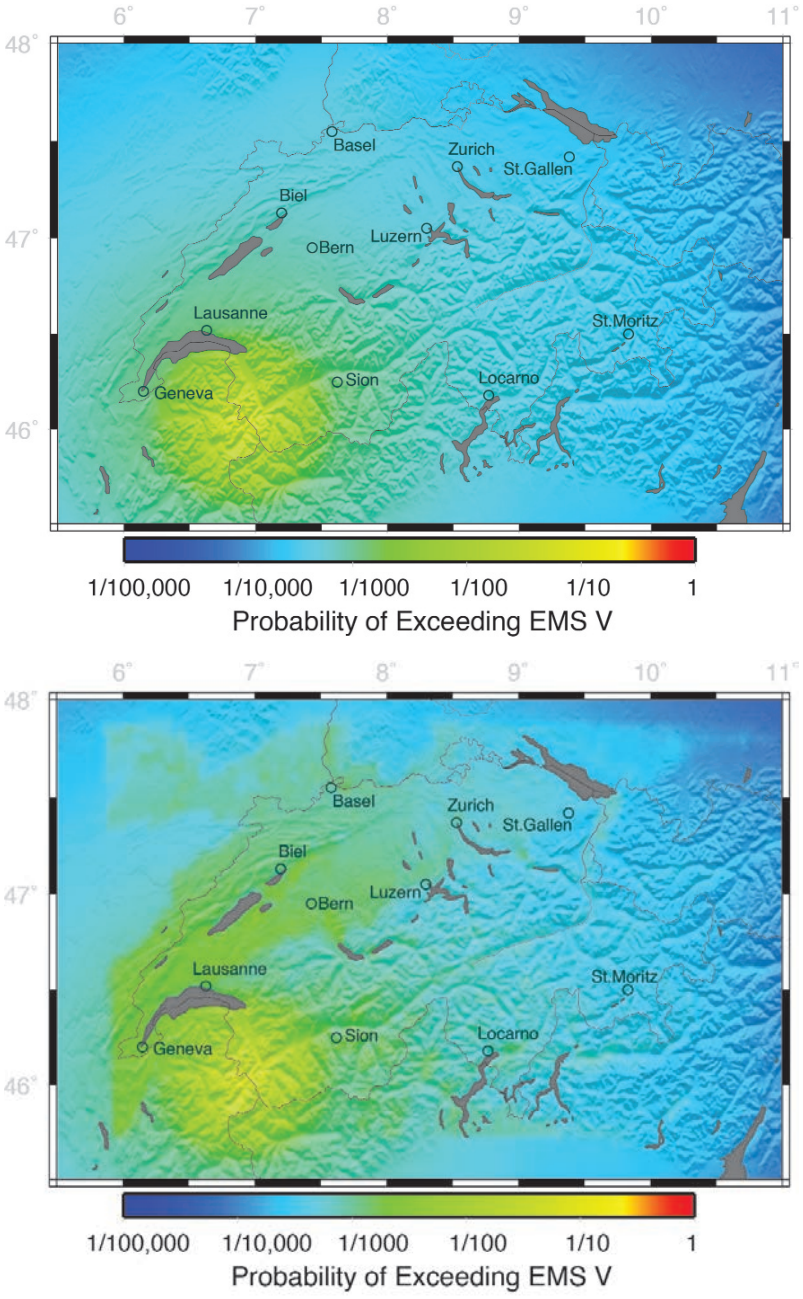


Fig. 8 - Snapshot of the STEP model for Switzerland for the September 2005 Vallorcine event. Forecasts are shown for the period September 9, 2005, 0:00 to September 10, 2005, 0:00. Maps are shown without (top) and with (bottom) site amplification (Kästli and Fäh, 2008).

best method to improve predictions for future events. This however needs calibration of the models with recordings of small earthquakes. Thus, one of the main goals of the project is to develop a detailed 3D velocity model of the area for realistic strong ground motion simulation.

The northern part of Visp is located in the Rhone valley, a Quaternary sedimentary basin consisting of horizontally-layered fluvial deposits (Roten *et al.*, 2006, 2008). The southern part is situated on complex formations of outcropping bedrock and alluvial deposits. A temporary seismic

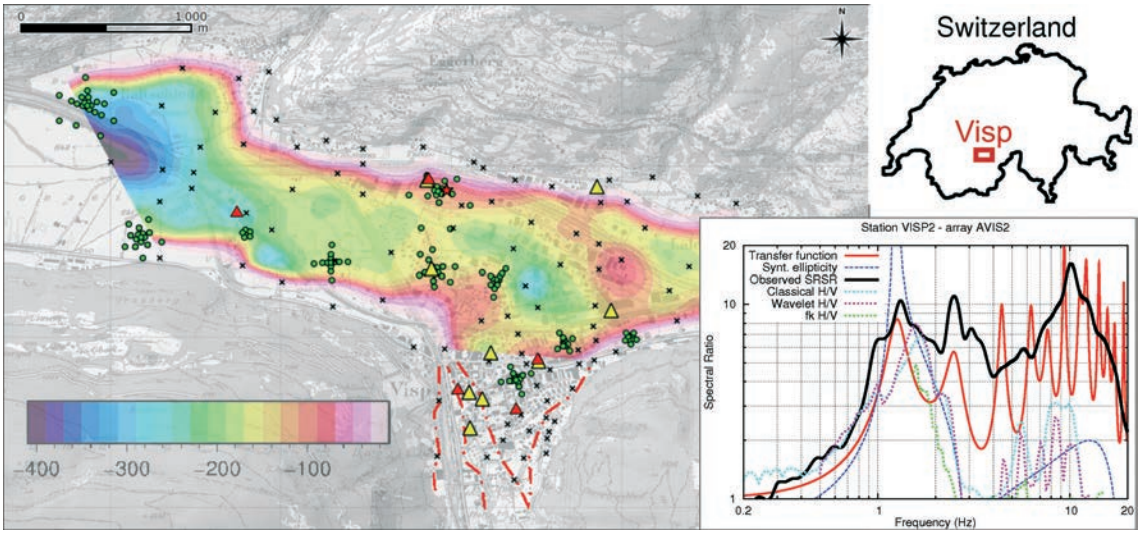


Fig. 9 - Overview of measurements performed in the Visp area. Location of the area is represented as a box on the map of Switzerland (top right). Ambient noise array measurements are shown as green dots, single-station measurements as black crosses, temporary stations as yellow triangles, and strong motion stations as red triangles. Color contour plot in the background represents the bedrock depth in the basin. Red dash-dot lines mark the area outside the basin where different sediment types are present. Right: comparison of observed mean site-to-reference spectral ratio (black), synthetic S-wave transfer function (red), ellipticity of the fundamental Rayleigh wave mode (blue), and three different methods for ellipticity estimation: 1) classical H/V method (cyan), 2) wavelet-based method (magenta), and 3) array-based method (green).

network was deployed during the winters of 2007-2008 and 2008-2009 to record weak ground motion due to local and regional earthquakes (Fig. 9). Seismic events recorded by this network were analyzed with classical site-to-reference spectral ratio methods (Borcherdt, 1970), resulting in an estimation of relative weak motion amplification. Amplification factors of up to 20 are observed at sites within the basin.

An extensive ambient noise measurement campaign was performed in the area (12 small-aperture arrays, almost 150 single-station measurements; see Fig. 9). The aim of array measurements was to constrain the average shear-wave velocity of main geological layers, identify key interfaces, and map lateral velocity variations. Single-station measurements were used to map changes in the interface depth between layers. Array measurements were processed by means of a three-component, high-resolution f-k method estimating both Love and Rayleigh dispersion curves (Fäh *et al.*, 2008). The ellipticity of Rayleigh waves was estimated by both new array-based (Poggi and Fäh, 2010) and wavelet-based techniques (Fäh *et al.*, 2009) for all array measurements. Locally, 1D velocity profiles were then obtained by joint inversion of the dispersion curves and Rayleigh wave ellipticities. One array was collocated with a deep borehole. Comparison between the inverted velocity profile and the borehole log shows good agreement, except for the bedrock interface (100 m depth at this site), which was not resolved by the array. Since the scatter of velocity profiles in the basin is not large, it was possible to define a reference profile by averaging the results from array surveys. Two strong interfaces are present in the reference profile: the first interface at around 50 m depth separates alternating silty, sandy and gravelly layers (S-wave

velocity <500 m/s) from underlying damaged rock or compacted sediments (S-wave velocity 900-1200 m/s). The second interface is the bedrock contact. Although the depth to bedrock could not be resolved from array measurements, its presence is necessary to explain the observed site-to-reference spectral ratios (Fig. 9). The depth of the first interface does not vary greatly throughout the study area (from 40-60 m). On the contrary, the depth to bedrock systematically increases towards the west, as estimated by inversion of resonant frequencies obtained from single station noise measurements (e.g., Poggi *et al.*, 2012).

### *6.2. Non-linear soil behavior and liquefaction*

To characterize the top-most stratigraphic layers in the valley, existing data from geotechnical and geological site investigations in the Visp area have been summarized (Mayor *et al.,* 2008; Roten *et al.*, 2009). These data show a primarily layered structure of the soil, which includes alternating gravel, sand and silt created by the meandering river of the Rhone. The first Rhone correction was performed at the end of the 19$^{th}$ century (DFI, 1964), and the position of the river and channel through the industrial area was fixed in 1905, allowing development of the area. The layered structure of the top-most soil units can be found throughout the entire valley while the thickness and distribution of the layers is highly variable. The silt and sand layers and lenses thereof have been identified prone to liquefaction based on gradation curves and SPT tests (Youd *et al.,* 2001). Most of the permeable materials are covered by fluvial sediments with high organic content. At the northern edge of the valley, the predominant material observed in borehole profiles is gravel. Information from the southern part of the study area is limited, although finer-grained material has been found at construction sites.

The influence of local soil stratigraphy on amplification and non-linear soil behavior (including pore pressure build up and strain-softening) will be studied with the planned borehole instrumentation (see Fig. 2). In addition, an extensive laboratory program is underway to determine the non-linear soil response in the alluvial silty-sand and establish relevant input parameters needed for non-linear soil models (e.g., Iai *et al.*, 1990). This program includes the study of the influence of the test procedure on the test results, which for example is important to judge softening of the soil due to pore pressure built up. Fig. 10 shows the development of pore pressures during undrained cyclic testing of two samples of silty sands from the Visp area. The sample shown at left is loaded by a 50 cycles of one load step followed by increase of the amplitude in subsequent cycles. This procedure of applying several load steps to one sample is usually adopted to cover sufficient loading scenarios for the determination of shear modulus and damping relationships with minimized laboratory efforts. Clearly this sequence causes a local change in stress state and density of the sample as shear zones or shear surfaces are activated. On the right hand side of Fig. 10, a sample is tested under similar boundary conditions, starting with one of the subsequent load steps (25 kPa) and pore pressures raised inside the sample to the value of the sample shown on the left after the second load step. In contrast to the sample at the left, no predefined shear zone exists. It is clear for this scenario that the increase in average pore pressure – shown as the ratio of $\Delta_u/\sigma'_{v0}$ - during the 50 cycles of the load step 25 kPa is significantly increased for the sample shown on the right. This increase is of special relevance for practical applications as it can lead to unsafe design using the common way of testing. Increase in pore water pressure, and thus softening, will be underestimated. This is of severe importance as the

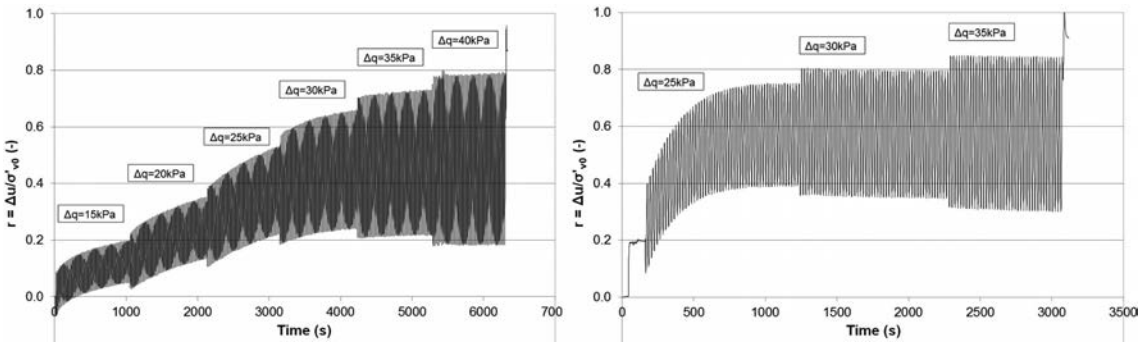


Fig. 10 - Development of liquefaction ratio during undrained cyclic testing of two samples from the Visp area. Left: sample loaded by 50 cycles starting with confining stresses of 15 kPa followed by subsequent increase of amplitude; right: sample tested under similar boundary conditions compared to the sample on the left, starting with the load values of the 25 kPa showing a significant difference of pore pressure increase for the amplitude of 25 kPa.

increase in pore water pressure develops faster in the first cycles and the number of cycles applied here exceeds the number of cycles to be expected during a magnitude 6.5 event. Nevertheless liquefaction hazard in the Visp area was analyzed in Roten *et al.* (2009), confirming observations of liquefaction reported after the 1855 $M_W$ 6.2 earthquake. This example shows the necessity of re-evaluating current laboratory procedures when defining liquefaction and softening due to pore pressure increase in real field situations.

### *6.3. Vulnerability assessment of buildings*

In order to evaluate the vulnerability of structures within the city of Visp, we performed a screening survey of the building stock. A database containing all survey parameters for approximately 360 buildings was created. The distribution of buildings is closely related to the history of the city. Visp used to be a small village located at a strategic point at the confluence of Vispa and Rhone rivers. Until the end of the 19$^{th}$ century, many houses were constructed of wood, while the houses of the townsmen were made of stone masonry with wooden floors. When the 1855 earthquake occurred, only rock outcrops and the alluvial fan were settled (Fritsche *et al.*, 2006). In 1909, the Lonza chemical industry was established in Visp, and the population and building stock grew in the direction of the Rhone plain. However, the new buildings were still made of stone masonry. Growth accelerated after 1945 and the entire Rhone valley was settled by the end of the 1970's. The new buildings were constructed of reinforced concrete (RC) walls or brick masonry with stiff floors. Seismic design appeared in the area only in 2004, when canton Valais made the Swiss building code SIA261 obligatory and began controlling design.

The screening survey showed that approximately two-thirds of the building stock consists of unreinforced masonry (URM) structures, half of them built of stone with wooden floors, the other half of brick, generally with stiff floors. Fewer than 30% of the structures are RC shear-wall buildings, 5% are wooden houses, and a few steel-frame industrial structures were noted. Most of the buildings are 2- to 3-stories high and only a few high-rise buildings are present.

The screened parameters allowed us to estimate the vulnerability of the building stock using different empirical methods proposed for Europe: a) the Risk-UE LM1 method (Lagomarsino and


Fig. 11 - Damage in Visp predicted for an intensity VIII earthquake using the Risk-UE LM1 method (Lagomarsino and Giovinazzi, 2006). Left: assuming rock site conditions; right: assuming strong site-effects induced by unconsolidated sediments.

Giovinazzi, 2006), and b) the Vulneralp method (Guéguen *et al.*, 2007). These methods compute both a vulnerability index for each structure and propose a relationship providing the mean damage grade as a function of the macroseismic intensity and vulnerability index. Since these methods are statistical, averages over selected quarters of the city were determined. A scenario of intensity VIII (Fig. 11) shows that these methods provide realistic results by comparison with the listed historical damages of the intensity VIII 1855 earthquake in the city centre on outcropping bedrock (Fritsche *et al.,* 2006). In order to predict the impact of future earthquakes, a more realistic distribution of ground motions in relation to the dynamic properties of the structures will be accounted for when numerical modeling results are finalized. Therefore, fragility functions were developed for the typical building types, especially URM. These were complemented by full-scale ambient vibration surveys in five buildings in Visp (more than 20 in Switzerland), performed by Michel *et al.* (2008), in order to estimate dynamic properties also accounting for non-linear behavior (Michel *et al.*, 2011). Using these new accurate data and models, more realistic scenarios will be analyzed in future work.

## 7. Rock slope triggering: test site Randa

The study region has a rich history of documented earthquake-induced rock slope failures. The most recent major earthquake and its aftershocks (1946 Sierre, $M_W$=5.8) triggered a number of landslides within the epicentral region and one large (~5 million m$^3$) rock avalanche (Fritsche and Fäh, 2009; Hunziker, 2011; Fritsche *et al.*, 2012). Similarly, widespread rockfall was described during the 1855 $M_W$=6.2 earthquake near St. Niklaus in the Matter valley (Fritsche *et al.*, 2006). One hundred years earlier in the same region, an estimated $M_W$=5.7 event triggered a ~1.5 million m$^3$ rock avalanche from the steep slopes above Niedergraechen, which ran out 2.7 km destroying part of the town (Noverraz *et al.*, 1998; Heynen, 2010). Earlier still, the strongest aftershock of the 1584 Aigle earthquake triggered a disastrous landslide covering the villages Corbeyrier and

Yvorne, in canton Vaud (Fritsche *et al.*, 2012).

Our study of earthquake-induced rock slope failures emphasizes both direct triggering and failure preparation through rock mass strength degradation. We back-analyze known failures, investigate the seismic response of existing instabilities, and install monitoring equipment to capture co- and post-seismic movements from different slopes. One main study site for our research is the Randa *in-situ* laboratory, established at the current rock slope instability above the village of Randa (Valais), where a slowly-moving volume of ~6 million $m^3$ (Fig. 12) remains following two catastrophic failures in 1991 (Gischig *et al.*, 2009, 2011). We employ ambient vibration measurements, analysis of ground motion recordings, and new fiber optic (FO) strain monitoring to measure the rock mass response to small regional earthquakes.

Ambient noise measurements revealed notable amplification of seismic energy within the unstable rock mass, with strong polarization in the direction of instability deformation (Burjanek *et al.*, 2010b). Site-to-reference spectral ratios up to 10 were identified for a frequency band around 5 Hz, polarized in the direction of movement. No polarization or amplification was observed outside of the unstable area. Results further highlighted resonant frequencies of internal rockslide blocks and of the larger unstable rock volume, caused by normal mode block vibration. This analysis was complemented with new measurements from two seismometers, which recorded continuous seismic data both inside and outside of the unstable area during seven small regional earthquakes in 2009. Amplifications within the instability zone reached factors of up to 7 for a frequency band centered around 3 Hz. Finally, we re-analyzed recordings of 80 regional earthquakes collected at Randa between 2002 and 2004 on a micro-seismic monitoring array (Spillmann *et al.*, 2007) with respect to local site-effects. Site-to-reference spectral ratios again revealed amplification factors up to ~5 within the unstable area, and polarization of the wave field in the direction of instability movement. Spectral peaks at ~3 Hz were observed for most stations within the instability, and ambient vibration measurements were confirmed at low frequencies.

FO strain sensors were installed as part of the COGEAR multi-sensor network in 2008 to measure co- and post-seismic deformation across key discontinuities at the surface and at depth (Moore *et al.*, 2010). These fiber Bragg grating sensors can measure micrometer-scale displacements at 100 Hz triggered sampling. On May 15, 2010, an earthquake of $M_W$=3.2 occurred about 5 km north of Randa at a focal depth of ~5 km. The earthquake triggered the FO system at Randa; data from the two surface crack extensometers (cracks Z9 and Z10, about 20 m apart) are presented in Fig. 13. The amplitude of fracture displacements reached peak values of around 50 μm, while no significant permanent offset was recorded. Spectral peaks from the FO strain record match closely with ambient vibration measurements and analysis of ground motion data recorded during previous experiments. Comparing strain records from either side of the instrumented block, two spectral peaks at 3 and 5 Hz were apparent. 5-Hz energy was found to be out-of-phase, as expected for normal mode vibration of a block between the two cracks, while 3-Hz energy was in-phase, representing the resonant frequency of the larger unstable rock mass (Fig. 12). 3-Hz resonance was also observed from previous seismic measurements throughout the unstable area, while 5-Hz peaks were visible only in the area of the instrumented crack.

The combined methodology offers new insight into the rockslide structure, highlighting effective block assemblages and offering clues as to their size. These analyses are complemented by high-resolution geodetic displacement monitoring and structural characterization, which

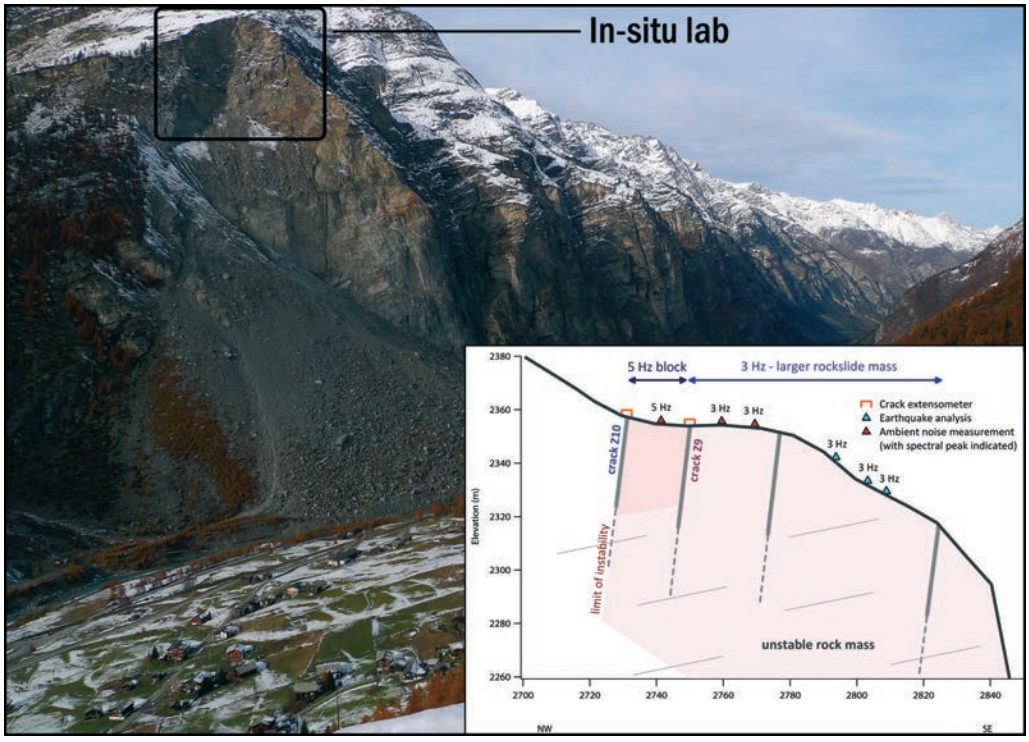


Fig. 12 - Randa rockslide and the location of the *in-situ* laboratory in the Matter valley (Valais). Inset: cartoon illustrating combined interpretation of deformation monitoring and ground motion recordings.

indicated 3-4 main block compartments within the upper part of the instability showing similar movement rates and orientations (Gischig *et al.*, 2011). Results of integrated studies also reveal significant site effects at Randa, which are not normally considered for rock slope instabilities. Our measurements suggest spectral amplification factors up to ~7 with strong polarization of the wave field, factors which may ultimately influence the potential for earthquake triggering. Such strong amplification cannot be explained by topographic site effects alone, i.e., only by the shape of the topography. We performed a number of numerical simulations which all required introduction of subsurface heterogeneity (compliant fractures, rock damage) to explain both observed resonant frequency and amplification (Burjanek *et al.*, 2011; Moore *et al.*, 2011).

## 8. Deep seated slope and soil triggering: test site Grächen

The village of Grächen is located on a morphological terrace at an altitude of 1600 m a.s.l. on the eastern flank of the Matter valley. The area is subject to very large-scale, low-amplitude displacement due to deep-seated sagging movement of the bedrock. The nature and amplitude of this displacement were investigated by Noverraz *et al.* (1998). This deep seated gravitational slope deformation is one of the largest known in the Alps, and has accumulated displacements of on average 300 mm between 1930 and 1992 (Fig. 14).

Potential earthquake-induced rock slope failures were investigated from the mountain slopes

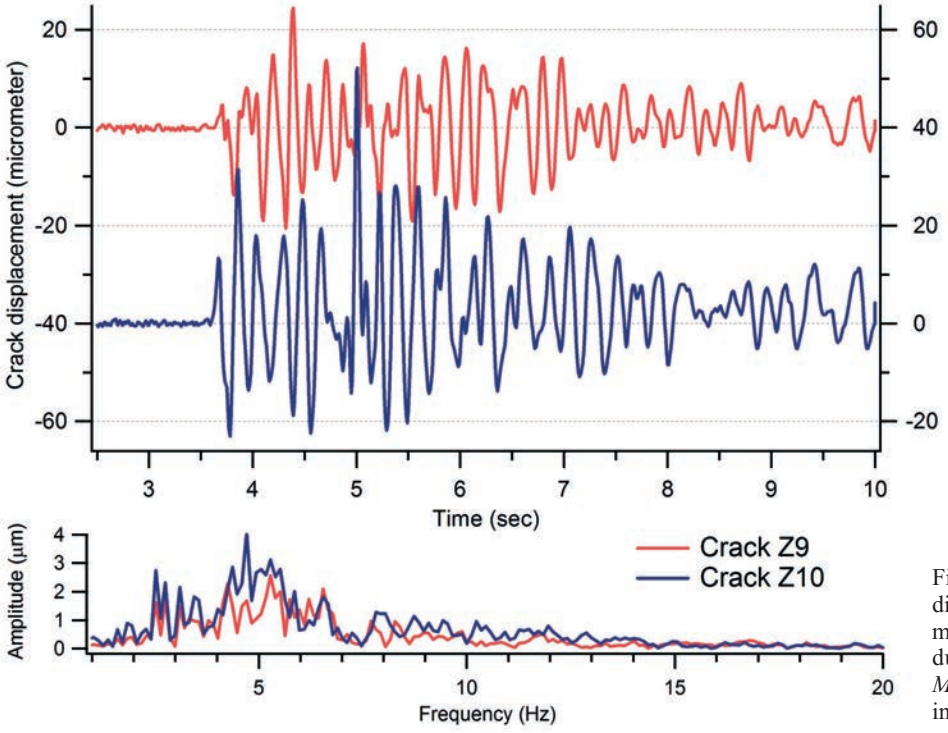


Fig. 13 - Crack displacements measured at Randa during the nearby $M_W$=3.2 earthquake in May 2010.

above the village of Grächen (Heynen, 2010). Our study analyzed different methods to predict co-seismic rock slope deformations considering both directional and topographic variations in ground motion. The results highlighted an interesting area of rock blocks at 'Platja' (Fig. 14) that appear to move only during periods of strong ground motion, and show displacements on the order of 1 m accumulated over the last ~20,000 years since exposure by deglaciation. The area is ideal for Newmark analysis, and the calculated co-seismic displacement of these blocks was comparable to the estimated movements using a number of representative earthquake input motions. Consultation of the historical record also uncovered a large rockslide triggered by the 1755 earthquake Noverraz *et al.*, 1998, which ran out over 2.7 km covering parts of the village of Niedergrächen (Fig. 14). Back analysis of the source area and deposit revealed a failed volume of roughly 1.5 million $m^3$, and a minimum horizontal acceleration needed to trigger failure in the range of 0.14 to 0.22 g (Heynen, 2010). In order to obtain an estimate of paleo-seismic peak ground acceleration (PGA) for the research area, a rocking / overturning analysis was carried out for selected precariously balanced rock blocks. The results indicate a predicted maximum past PGA of ~0.4 g, which is in accordance with shaking intensity estimates from previous earthquakes.

Earthquake site-effects related to soil layers at the Grächen site were also analyzed. Four existing drilling data sets were gathered (see Fig. 14) and used to investigate the nature and thickness of soil deposits in the Grächen area (Eichenberger *et al.*, 2010). Soil thickness varies greatly but is primarily between 50 and 100 m; the maximum thickness being located in the southern part of the village. One borehole was drilled in the rock avalanche deposit, which has a thickness of 7 m at that point. The drillings reveal a soil column that consists primarily of moraine

and lacustrine deposits with abundant large rock blocks. In terms of granulometry, main soil types can be classified as silty-sand with blocks. Soil permeability is low except where talus is encountered. A ~10 m thick, fine-grained deposit with very low permeability containing no blocks was identified at around 30 m depth.

The influence of earthquakes on observed and predicted shallow landslides must be estimated. Field analysis of shallow slope movements revealed the most important factor in observed landslides is water input from nearby drainage channels. The silty soil is then saturated and cohesionless, which combined with locally steeper slope gradients explains the shallow landslide occurrence. While such slides may show activity during an earthquake, their small size and localized origin makes them a lesser concern for the area. The presence of thick layers of alluvial deposits, however, may be problematic in a strong earthquake due to amplification of seismic waves. Compared to those of the Rhone valley, these deposits are not as fine grained and are mainly dry. 1D dynamic analysis was performed for two soil columns representing the village location, for preliminary assessment of amplification (without 2D/3D site-effects). The first profile reaches bedrock at 50 m depth, while the second is 76 m deep. Elastic properties were estimated from ambient noise array measurements (Burjanek *et al.*, 2010a). Due to the nature of the soil, we used a non-linear material model to describe the soil response; Hujeux's model (Aubry *et al.*, 1982) was selected for its ability to model both coarse- and fine-grained soils. Using as input motion a recording from a magnitude 5.8 earthquake in Costa Rica in 1993, spectral amplification factors reach values of about 2 to 3 for both soil profiles (Fig. 14).

## 8. Summary and conclusion

Project COGEAR represents a unique interdisciplinary endeavor for Switzerland, tackling relevant scientific and socio-economic topics. Earthquakes regularly claim large number of lives and result in high economic losses. Mitigation and understanding of the coupled hazard chain is therefore of paramount importance, especially in countries such as Switzerland where seismicity is moderate but possible impacts are often not fully appreciated. Common underestimation of seismic hazard is due to the infrequent but nonetheless inevitable reoccurrence of powerful, damaging earthquakes; based on the approximate 100-year recurrence rate in the Valais, a damaging earthquake is expected within two generations.

COGEAR has initiated a multi-level interdisciplinary research program to address the issue of earthquake related hazards. A number of topical meetings has been organized in order to establish common infrastructure and long-term goals for scientific research through cooperation and coordination. In relation to COGEAR's infrastructure, the integration and accessibility of new seismological-relevant data sets and the well-structured and organized distributed databases is an important achievement, and sets the standard for future data collection, storage and organization. The common monitoring systems provide access to a variety of new sensors, which has already stimulated new research avenues. If we can sustain the common monitoring systems, we can guarantee collaboration beyond the duration of the project with continued merging of unique data sets. Finally, essential collaboration with project partners has allowed creation of new research fields investigating different aspects of seismogenic hazards.

Scientific work is in progress and we expect additional results relevant for stakeholders,

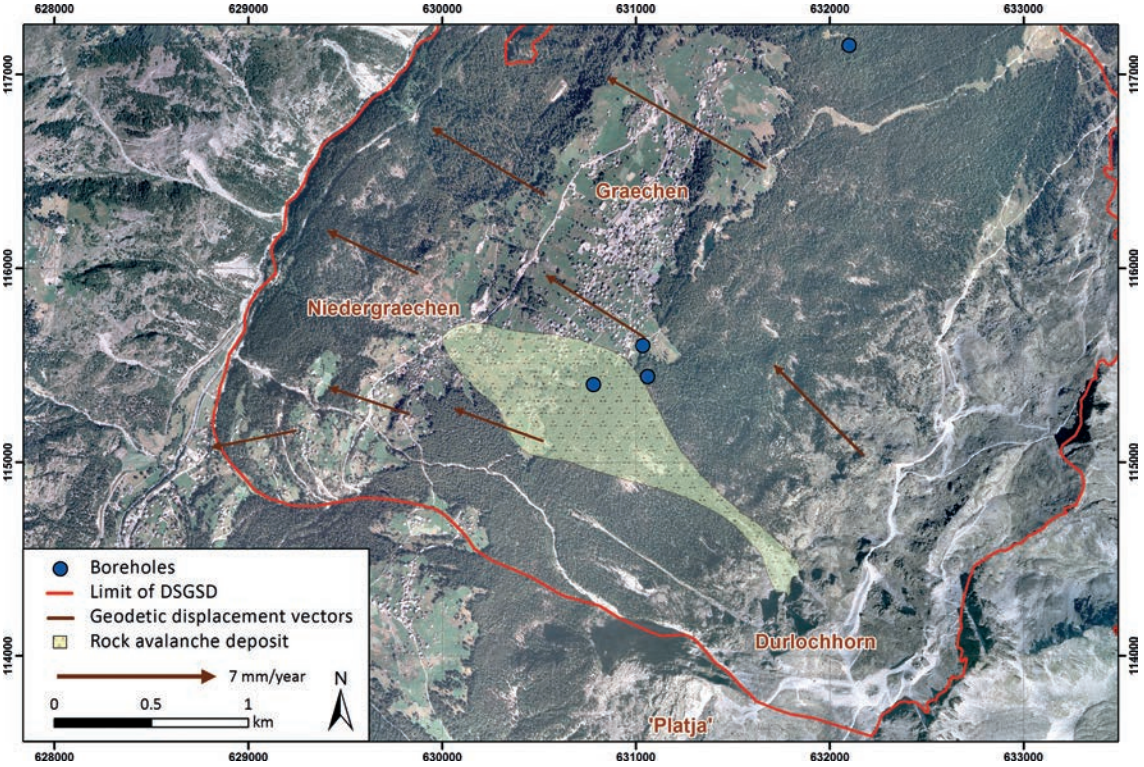


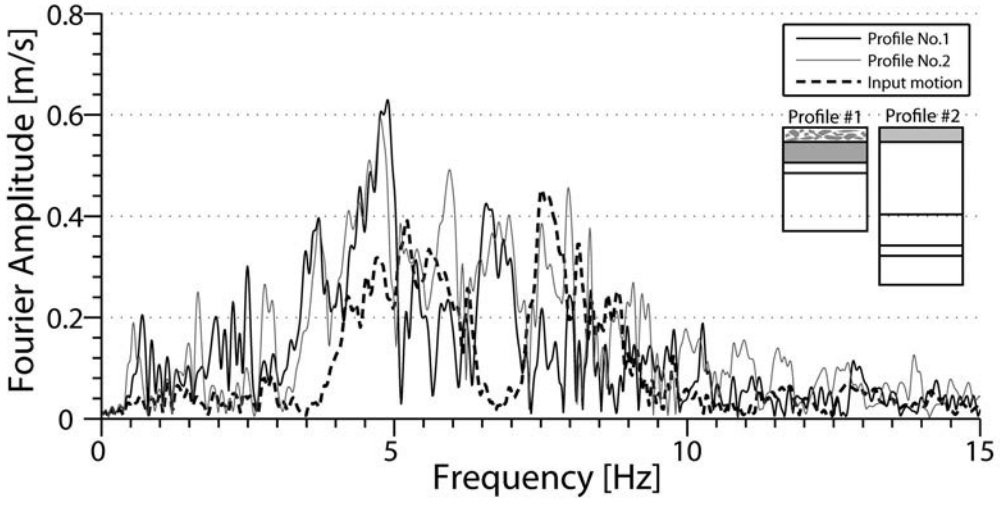


Fig. 14 - Top: overview of the Grächen area showing deposit of the 1755 Niedergrächen earthquake-induced rock avalanche (shaded yellow) and the source area at Durlochhorn (Heynen, 2010). Shaded circles indicate the location of boreholes with soil profile information. Brown arrows show the magnitude and orientation of geodetic displacement measurements over a 62 year period (Noverraz *et al.,* 1998). Swiss coordinates are in meters. Bottom: Fourier amplitude spectra of ground acceleration at the top of two profiles from Grächen, including bedrock motion for reference. Moraine till is shown in grey, lacustrine deposits in white.

engineers, and the public alike. Due to strong urban development in the last century and growth of cities into increasingly vulnerable areas, future earthquakes will cause more damage than has yet been observed. For this reason, it is crucial to recognize and map potential areas of large earthquake impact, estimate ground motion and non-linear effects, and provide adequate estimates of ground motion for reliable spectra in building codes.

**Acknowledgements.** The authors would like to thank S. Grimaz and D. Slejko, and an anonymous reviewer for constructive comments and helpful suggestions. This research is part of the projects COGEAR and SwissExperiment, both funded by the Competence Center for Environment and Sustainability of the ETH Domain (CCES).

## REFERENCES

Aubry D., Hujeux J.-C., Lassoudière F. and Meymon Y.; 1982: *A double memory model with multiple mechanisms for cyclic soil behaviour*. In: Proc. 1st Int. Symp. Numer. Models Geomech., Zurich, Switzerland, pp. 3-13.

Ben-Zion Y., Peng Z., Lewis M.A. and McGuire J.; 2007: *High resolution imaging of fault zone structures with seismic fault zone waves*. Sci. Drill., Special Issue. **1**, 78-79, doi:10.2204/iodp.sd.s01.23.2007.

Borcherdt R.D.; 1970: *Effects of local geology on ground motion near San Francisco Bay*. Bull. Seismol. Soc. Am., **60**, 29-61.

Burjanek J., Gassner-Stamm G. and Fäh D.; 2010a: *Array-measurements in the area of Visp and St. Niklaus*. COGEAR, 3.1.2, Swiss Seismological Service (SED), 77 pp.

Burjanek J., Gassner-Stamm G., Poggi V., Moore J.R. and Fäh D.; 2010b: *Ambient vibration analysis of an unstable mountain slope*. Geophys. J. Int., **180**, 820-828.

Burjanek J., Moore J.R., Gassner-Stamm G. and Fäh D.; 2011: *Seismic response of unstable mountain rock slopes: topographic site effect?*. In: Proc. 4th IASPEI/IAEE Int. Symp., Effects of Surface Geology on Seismic Motion, Santa Barbara, CA, USA, 11 pp.

Carto.net; 2011: www.carto.net, last access Feb. 2011.

Christophersen A. and Gerstenberger M.C.; 2010: *A new generic model for aftershock decay in earthquake forecasting*. Seismol. Res. Lett., **81**, 316.

Dach R., Hugentobler U., Fridez P. and Meindl M. (eds); 2007: *Bernese GPS Software Version 5.0*. Astron. Inst., University of Bern, Switzerland, 636 pp.

DFI (Departement Federal de l'Interieur); 1964: *La correction du Rhone en amont du lac Lemon*, Bern.

Eckerson W.W.; 1995: *Three tier client/server architecture: achieving scalability, performance, and efficiency in client server applications*. Open Inf. Syst., **10**, 1-20.

Eichenberger J., Ferrari A., Schurmann C. and Laloui L.; 2010: *Overview of existing data in the Matter valley (soil slopes)*. COGEAR, 3b.3.1, EPFL, 7 pp.

Fäh D., Giardini D., Bay F., Bernardi F., Braunmiller J., Deichmann N., Furrer M., Gantner L., Gisler M., Isenegger D., Jimenez M.-J., Kästli P., Koglin R., Masciadri V., Rutz M., Scheidegger C., Schibler R., Schorlemmer D., Schwarz-Zanetti G., Steimen S., Sellami S., Wiemer S. and Wössner J.; 2003: *Earthquake catalogue of Switzerland (ECOS) and the related macroseismic database.* Eclogae Geol. Helv., **96**, 219-236.

Fäh D., Giardini D., Kästli P., Deichmann N., Gisler M., Schwarz-Zanetti G., Alvarez-Rubio S., Sellami S., Edwards B., Allmann B., Bethmann F., Wössner J., Gassner-Stamm G., Fritsche S. and Eberhard D.; 2011: *ECOS-09, Earthquake catalogue of Switzerland: release 2011*. Swiss Seismological Service, ETH Zurich, Report SED/RISK/R/001/20110417, 42 pp.

Fäh D., Stamm G. and Havenith H.-B.; 2008: *Analysis of three-component ambient vibration array measurements*. Geophys. J. Int., **172**, 199-213.

Fäh D., Wathelet M., Kristekova M., Havenith H.-B., Endrun B., Stamm G., Poggi V., Burjanek J. and Cornou C.; 2009:

*Using ellipticity information for site characterisation*. NERIES JRA4 "Geotechnical Site Characterization", task B2-D4, final report, 54 pp.

Fréchet J., Thouvenot F., Frogneux M., Deichmann N. and Cara M.; 2011: *The Mw 4.5 Vallorcine (French Alps) earthquake of 8 September 2005 and its complex aftershock sequence.* J. Seism., **15**, 43-58, doi:10.1007/s10950-010-9205-8.

Fritsche S. and Fäh D.; 2009: *The 1946 magnitude 6.1 earthquake in the Valais: Site-effects as contributor to the damage*. Swiss J. Geosci., **102**, 423-439.

Fritsche S., Fäh D., Gisler M. and Giardini D.; 2006: *Reconstructing the damage field of the 1855 earthquake in Switzerland: historical investigations on a well-documented event.* Geophys. J. Int., **166**, 719-731.

Fritsche S., Fäh D. and Schwarz-Zanetti G; 2012: *Historical intensity VIII earthquakes along the Rhone valley (Valais, Switzerland): Primary and secondary effects*. Swiss J. Geosci., **105**, 1-18.

Gasperini P. and Lolli B.; 2006: *Correlation between parameters of the aftershock rate equation: implications for the forecasting of future sequences*. Phys. Earth Planet. Int., **156**, 41-58.

GeoVITe; 2011: *Website of geodata visualization and interactive training environment (GeoVITe)*. http://geodata.ethz.ch/geovite/, last access Feb. 2011.

Gerstenberger M.C., Wiemer S., Jones L.M. and Reasenberg P.A.; 2005: *Real-time forecasts of tomorrow's earthquakes in California.* Nature, **435**, 328-331, doi:10.1038/nature03622.

Gischig V., Amann F., Moore J.R., Loew S., Eisenbeiss H. and Stempfhuber W.; 2011: *Composite rock slope kinematics at the current Randa instability, Switzerland, based on remote sensing and numerical modelling*. Eng. Geol., **118**, 37-53.

Gischig V., Loew S., Kos A., Moore J.R., Raetzo H. and Lemy F.; 2009: *Identification of active release planes using ground-based differential InSAR at the Randa rock slope instability, Switzerland*. Nat. Hazards Earth Syst. Sci., **9**, 2027-2038.

Gogu R.C., Dietrich V.J., Jenny B., Schwandner F.M. and Hurni L.; 2006: *A geo-spatial data management system for potentially active volcanoes*. Computer & Geosciences, **32**, 29-41.

Guéguen P., Michel C. and Le Corre L.; 2007: *A simplified approach for vulnerability assessment in moderate-to-low seismic hazard regions: application to Grenoble (France).* Bull. Earthquake Eng., **5**, 467-490.

Heynen M.; 2010: *Einfluss lokaler Geländegegebenheiten auf die seismische stabilität eines Felshanges (Seetalhorn, VS).* M.Sc. Thesis in Engineering Geology, ETH Zurich, 108 pp.

Hollenstein Ch., Muller M.D., Geiger A. and Kahle H.-H.; 2008*: Crustal motion and deformation in Greece from a decade of GPS measurements*, *1993-2003*. Tectonophys., **449**, 17-40, doi:10.1016/j.tecto.2007.12.006.

Hunziker M.; 2011: *Earthquake-induced rock slope failures: the 1946 Rawilhorn rock avalanche.* M.Sc. Thesis in Engineering Geology, ETH Zurich, 55 pp.

Iai S., Matsunaga Y. and Kameoka T.; 1990: *Parameter identification of a cyclic mobility model*. Rep. Port and Harbour Res. Inst., **29**, 57-83.

Iosifescu I. and Hurni L.; 2010: *GIS Platform for interdisciplinary environmental research*. In: Proc. 7th ICA Mountain Cartography Workshop, Borsa, Romania, Geographia Technica, Spac. Issue, pp. 52-64.

Iosifescu I., Hugentobler M. and Hurni L.; 2010: *Web cartography with open standards – A solution to cartographic challenges of environmental management*. Environ. Modell. Softw., **25**, 988-999.

Kästli P. and Fäh D.; 2008: *Earthquake scenarios for the Basel area based on macroseismic intensities.* In: Evaluation of the induced seismicity in Basel 2006/2007: locations, magnitudes, focal mechanisms, statistical forecasts and earthquake scenarios, Swiss Seismological Service, Zürich.

Kastrup U., Zoback M.-L., Deichmann N., Evans K., Giardini D. and Michael A.J.; 2004: *Stress field variations in the Swiss Alps and the northern Alpine foreland derived from inversion of fault plane solutions*. J. Geophys. Res., **109**, B01402, doi:10.1029/2003JB002550.

Lagomarsino S. and Giovinazzi S.; 2006: *Macroseismic and mechanical models for the vulnerability and damage assessment of current buildings*. Bull. Earthquake Eng., **4**, 415-443.

Maurer H. and Deichmann N.; 1995: *Microearthquake cluster detection based on waveform similarities, with an application to the western Swiss Alps.* Geophys. J. Int., **123**, 588-600.

Maurer H., Burkhard M., Deichmann N. and Green A.G.; 1997: *Active tectonism in the western Swiss Alps.* Terra Nova, **9**, 91-94.

Mayor P.A., Springman S.M. and Teysseire P.; 2008: *In situ field experiment to apply variable high water levels to a river levee*. In: Toll D.G. (ed), Unsaturated soils. Advances in Geo-Engineering, Taylor & Francis Group, London, ISBN 978-

0-415-47692-8, pp. 947-952.

Michel C., Guéguen P. and Bard P-Y.; 2008: *Dynamic parameters of structures extracted from ambient vibration measurements: An aid for the seismic vulnerability assessment of existing buildings in moderate seismic hazard regions*. Soil Dyn. Earthquake Eng., **28**, 593-604.

Michel C., Zapico B., Lestuzzi P., Molina F.J. and Weber F.; 2011: *Quantification of fundamental frequency drop for unreinforced masonry buildings from dynamic tests*. Earthquake Eng. Struct. Dyn., **40**, 1283-1296.

Moore J.R., Gischig V., Burjanek J., Loew S. and Fäh D.; 2011: *Site effects in unstable rock slopes: dynamic behavior of the Randa instability (Switzerland)*. Bull. Seismol. Soc. Am., **101**, 3110-3116, doi:10.1785/0120110127.

Moore J.R., Gischig V., Button E. and Loew S.; 2010: *Rockslide deformation monitoring with fiber optic strain sensors*. Nat. Hazards Earth Syst. Sci., **10**, 191-201.

Noverraz F., Bonnard C., Dupraz H. and Huguenin L.; 1998: *Grands glissements de terrain et climat, VERSINCLIM - Comportement passé, présent et futur des grands versants instables subactifs en fonction de l'évolution climatique, et évolution en continu des mouvements en profondeur.* Rapport final PNR31 (Programme National de Recherche), ETH Zürich, Switzerland, 314 pp.

Ogata Y.; 1988: *Statistical models of earthquake occurrences and residual analysis for point processes*. J. Am. Stat. Assoc., **83**, 9-27.

Poggi V. and Fäh D.; 2010: *Estimating Rayleigh wave particle motion from three-component array analysis of ambient vibrations*. Geophys. J. Int., **180**, 251-267.

Poggi V., Fäh D., Burjanek J. and Giardini D.; 2012 : *The use of Rayleigh wave ellipticity for site-specific hazard assessment and microzonation. Application to the city of Lucerne, Switzerland*. Geophys. J. Int., **188**, 1154-1172, doi:10.1111/j.1365-246X.2011.05305.x.

PostgreSQL; 2011: *Website of the open source object-relational database system PostgreSQL*. www.postgresql.org/, last access Feb. 2011.

QGIS mapserver; 2011: *Website of QGIS mapserver.* http://karlinapp.ethz.ch/qgis_wms/index.html, last access Feb. 2011.

Roten D., Fäh D., Bonilla F., Alvarez-Rubio S., Weber T. and Laue J.; 2009: *Estimation of nonlinear site response in a deep Alpine valley*. Geophys. J. Int., **178**, 1597-1613.

Roten D., Fäh D., Cornou C. and Giardini D.; 2006*: 2D resonances in Alpine valleys identified from ambient vibration wavefields*. Geophys. J. Int., **165**, 889-905.

Roten D., Fäh D., Olsen K.B. and Giardini D.; 2008: *A comparison of observed and simulated site response in the Rhone valley*. Geophys. J. Int., **173**, 958-978.

Spillmann T., Maurer H., Green A.G., Heincke B., Willenberg H. and Husen S.; 2007: *Microseismic investigation of an unstable mountain slope in the Swiss Alps*. J. Geophys. Res., **112**, B07301, doi:10.1029/2006JB004723.

Wiemer S., Giardini D., Fäh D., Deichmann N. and Sellami S.; 2008: *Probabilistic seismic hazard assessment of Switzerland: best estimates and uncertainties*. J. Seismolog., **13**, doi:10.1007/s10950-008-9138-7.

Woessner J., Christophersen A., Zechar J.D. and Monelli D.; 2010: *Building self-consistent, short-term earthquake probability (STEP) models: improved strategies and calibration procedures*. Ann. Geophys., **53**, doi:10.4401/ag-4812.

Woessner J., Hainzl S., Marzocchi W., Werner M.J., Lombardi A.M., Catalli F., Enescu B., Cocco M., Gerstenberger M.C. and Wiemer S.; 2011: *A retrospective comparative forecast test on the 1992 Landers sequence*. J. Geophys. Res., **116**, B05305, doi:10.1029/2010JB00784.

Youd T.L., Idriss I.M., Andrus R.D., Arango I., Castro G., Christian J.T., Dobry R., Finn W.D.L., Harder L.F.J., Hynes M.E., Ishihara K., Koester J.P., Liao S.S.C., Marcuson III W.F., Martin G.R., Mitchell J.K., Moriwaki Y., Power M.S., Robertson P.K., Seed R.B. and Stokoe II K.H.; 2001: *Liquefaction resistance of soils:summary report from the 1996 NCEER and 1998 NCEER/NSF Workshops on evaluation of liquefaction resistance of soils*. J. Geotech. Geoenviron. Eng., **127**, 817-833.

*Corresponding author:* Donat Fäh
ETH Zürich, Swiss Seismological Service
Sonneggstrasse 5, 8092 Zürich, Switzerland
Phone: +41 44 6332658, e-mail: donat.faeh@sed.ethz.ch.